Saturation spectroscopy for optically thick atomic samples

Svanberg, Sune; Yan, G.Y.; Duffey, T.P.; Du, W. M.; Hänsch, T. W.; Schawlow, A. L.

Published in:
Journal of the Optical Society of America B: Optical Physics

DOI:
10.1364/JOSAB.4.000462

1987

Saturation spectroscopy for optically thick atomic samples

S. Svanberg, G.-Y. Yan, T. P. Duffey, W.-M. Du,* T. W. Hänsch, and A. L. Schawlow

Department of Physics, Stanford University, Stanford, California 94305

Received Oct 13, 1986; accepted November 25, 1986

Doppler-free saturation spectroscopy in the regime of strong pumping intensities and optically thick atomic samples is investigated experimentally and theoretically. It is shown that a very high signal-to-background ratio can be obtained and, at the same time, subnatural linewidths can be reached. Further contrast and linewidth improvements can be attained by supplementing the primary depleted pumping beam with a second pumping beam. By using the signal beam from a first setup as the pumping beam for a second identical arrangement, extreme values for contrast and linewidth should be attainable.

INTRODUCTION

We have recently[1] demonstrated how Doppler-free saturation spectroscopy in the regime of strong pumping intensity and high integrated sample absorption yields strong, narrow signals on an essentially zero background. In this paper we present a theoretical description of the phenomena as well as further experimental data on the technique, which we have denoted high-contrast transmission spectroscopy. We also describe how further improvements in signal-to-background ratio (contrast) and linewidth reduction can be obtained by injecting an additional pumping beam or by running two identical setups in series.

The saturation spectroscopy technique employing dye lasers was introduced by Hänsch *et al.*[2] In order to avoid power broadening of the Doppler-free signals, normally modest pump-beam intensities are used. At the line center only a small fractional change in the transmitted probe-beam intensity is then obtained for samples typically absorbing half the probe-beam light. The situation is very different in the high-intensity, high-absorption regime, in which the probe-beam transmission can increase from essentially zero to several tens of percent of its unattenuated value. Because of the exponential nature of the Beer–Lambert law of absorption, the wings of the Doppler-free signal are more strongly absorbed than the central part. This effect can be made to dominate over the power broadening, and linewidths below the natural radiation width limit can be obtained for isolated signal components.

Two different experimental arrangements for high-contrast transmission spectroscopy are shown in Fig. 1. In Fig. 1(a) a conventional setup for saturation spectroscopy is shown. In the high-contrast version it is important for the weak probe beam to overlap with the strong pump beam over the entire length of the absorption cell. Therefore the probe beam is detected through a semitransparent folding mirror. In Fig. 1(b) a simplified version of the setup is shown. The primary beam is sent through a beam splitter and forms a strong pumping beam traversing the cell. It is strongly absorbed despite considerable sample bleaching, and the retroreflected beam forms a weaker probe beam that is reflected off the beam splitter. The intensity falloff for the pump beam traversing the cell is indicated as well as the gradual change in the absorption coefficient.

As first illustrations, signals obtained for the sodium D_1 ($3\,^2S_{1/2}$–$3\,^2P_{1/2}$) and D_2 ($3\,^2S_{1/2}$–$3\,^2P_{3/2}$) lines in experiments employing the setup in Fig. 1(a) are shown in Figs. 2(a) and 2(b), respectively. Experimental details will be presented later. For the samples that are normally almost opaque to the weak probe beam (linear absorption) in the central parts of the Doppler-broadened profile, sharp Doppler-free transmission peaks corresponding to hyperfine structure (hfs) transitions are observed. The relevant hfs of the two D lines is also given in the figure. For the D_1 line the excited-state hfs splitting of 189 MHz is clearly resolved, and the crossover resonances[3] are also obtained. The upper-state hfs is too small to be resolved at the power level used for the D_2 line recording. The favorable signal-to-background ratio obtained resembles that obtainable in polarization spectroscopy[4] but is achieved without the use of polarizers. As in fluorescence monitoring, a strong signal is observed when the resonance condition is fulfilled, but otherwise no light is observed.

After this brief introduction of the basic high-contrast transmission spectroscopy scheme we will present a simple theoretical modeling of the experiment in the next section and also make some qualitative comparisons between experiment and theory; then a repumping scheme for further contrast enhancement is analyzed theoretically and demonstrated experimentally. In a further section before the final discussion, a tandem scheme involving two coupled experimental arrangements is analyzed, illustrating possibilities for extreme contrast improvement and linewidth reduction.

BASIC SINGLE-CELL VERSION

Theoretical Modeling

We will present here a simple hole-burning description of the saturation spectroscopy experiment in the regime of high integrated optical absorption. Effects caused by dynamic Stark interaction, self-focusing, etc. are neglected. We consider a pump (saturating) beam of initial intensity $I(0)$ impinging upon a Doppler-broadened atomic sample of length L. The sample, with a particular number density of atoms of absorption oscillator strength f, exhibits a linear absorption coefficient α_0 for weak monochromatic light. The transition will be saturated for higher intensities, lead-

0740-3224/87/040462-08$02.00

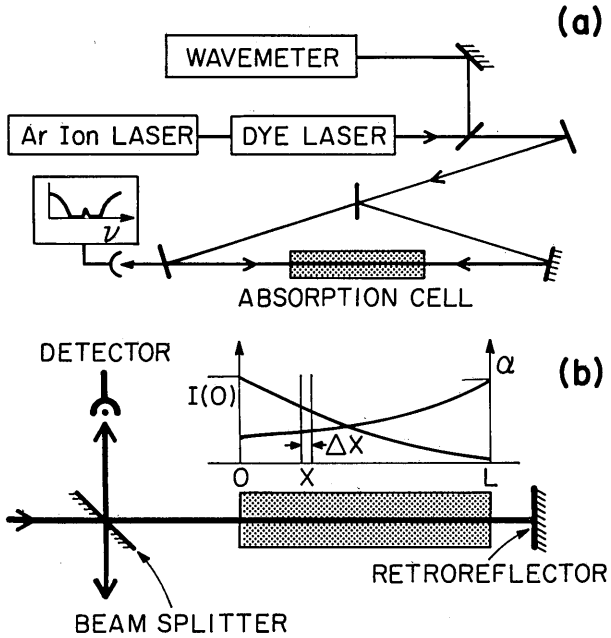

Fig. 1. Experimental arrangements for high-contrast transmission spectroscopy. (a) Arrangement with separate probe beam of constant power. (b) Simplified arrangement in which the attenuated pump beam is used as the probe beam.

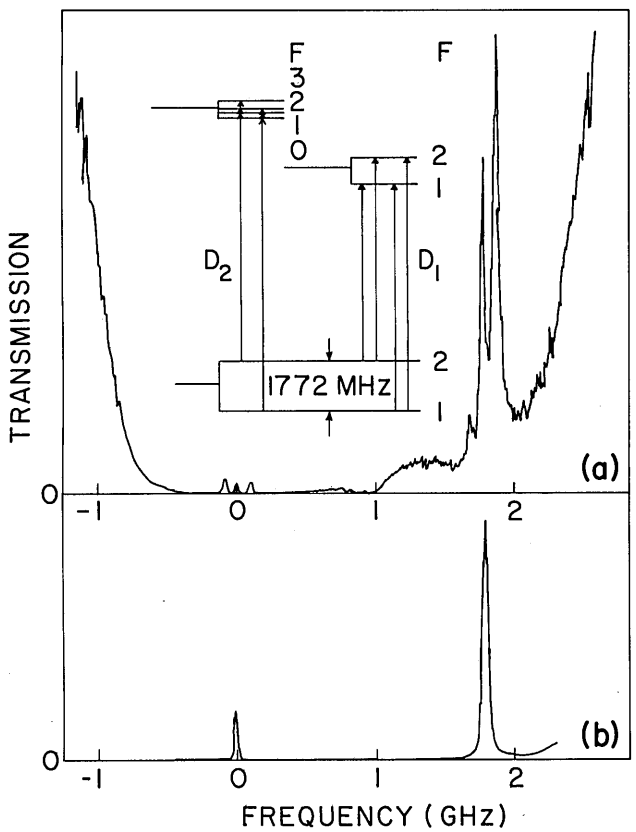

Fig. 2. Recordings for the sodium D lines and relevant transition hyperfine-structure diagrams. (a) D_1 line recording, using a 10-cm cell at 155°C. The probe-beam intensity is 8% of the pump beam intensity. (b) D_2 line recording, using a 30-cm cell at 141°C. The probe beam intensity is 0.5% of the pump beam intensity.

ing to bleaching of the sample; i.e., the absorption coefficient will be reduced:

$$\alpha = \alpha_0/\sqrt{1 + I/I_{\text{sat}}}, \tag{1}$$

where I_{sat} is the saturation intensity.[5]

For a strongly absorbing sample the remaining normalized intensity $I(x)/I_{\text{sat}}$ at a penetration depth x into the cell is obtained by integration:

$$I(x)/I_{\text{sat}} = I(0)/I_{\text{sat}} \exp\left[-\int_0^x \alpha(x')\mathrm{d}x'\right]. \tag{2}$$

Here $\alpha(x')$ continuously increases through the sample according to Eq. (1) as $I(x)/I_{\text{sat}}$ is reduced. The inhomogeneously broadened hole in the velocity distribution of the atoms in a slice Δx of the sample will be described by a Lorentzian with a linewidth $\Delta\nu$ that is larger than the natural width $\Delta\nu_N = \frac{1}{2}\pi\tau$ (τ is the lifetime of the excited state) because of the power broadening[5]:

$$\Delta\nu = \tfrac{1}{2}\Delta\nu_N(1 + \sqrt{1 + I/I_{\text{sat}}}). \tag{3}$$

At the position x along the pump beam the effective frequency-dependent absorption coefficient for a weak, counterpropagating beam will be

$$\alpha_\nu(x) = \alpha_0 - \frac{\alpha_0 - \alpha(x)}{1 + \left(\dfrac{\nu - \nu_0}{\Delta\nu/2}\right)^2}, \tag{4}$$

where $\alpha(x)$ is calculated from Eq. (1) using the I/I_{sat} value obtained from Eq. (2). The resulting probe-beam transmission T_ν through the sample is obtained by integration of Eq. (4) over the cell length L:

$$T_\nu = \exp\left[-\alpha_0 L + \int_0^L \frac{\alpha_0 - \alpha(x)}{1 + \left(\dfrac{\nu - \nu_0}{\Delta\nu/2}\right)^2}\mathrm{d}x\right]. \tag{5}$$

The contrast C is the ratio of the Doppler-free signal peak transmission (background free) to the background transmission [far from resonance, $T_{\text{off-res}} = \exp(-\alpha_0 L)$]:

$$C = \exp\left[\int_0^L -\alpha(x)\mathrm{d}x + \alpha_0 L\right] - 1. \tag{6}$$

We have calculated the transmission T_ν, the contrast C, and the resulting linewidth, numerically integrating Eqs. (2), (5), and (6) by dividing the cell length into 50 equal intervals. The calculations were performed on an IBM PC XT, using a FORTRAN program. The results are shown in Fig. 3 as a function of integrated linear absorption coefficient $\alpha_0 L$ for three values of $I(0)/I_{\text{sat}}$: 10, 30, and 100. It is clearly shown how the probe beam can penetrate the sample increasingly effectively by using the path bleached by a pump beam of increasing intensity through the otherwise optically thick sample. The contrast increases with increasing pump power, increases with optical density, and finally levels off. For the case of strong initial saturation and very dense samples, an approximate analytical expression for this maximum contrast can easily be derived:

$$C_{\text{lim}} \approx \frac{4\exp(2\sqrt{1 + I/I_{\text{sat}}} - 2)}{(1 + \sqrt{1 + I/I_{\text{sat}}})^2}. \tag{7}$$

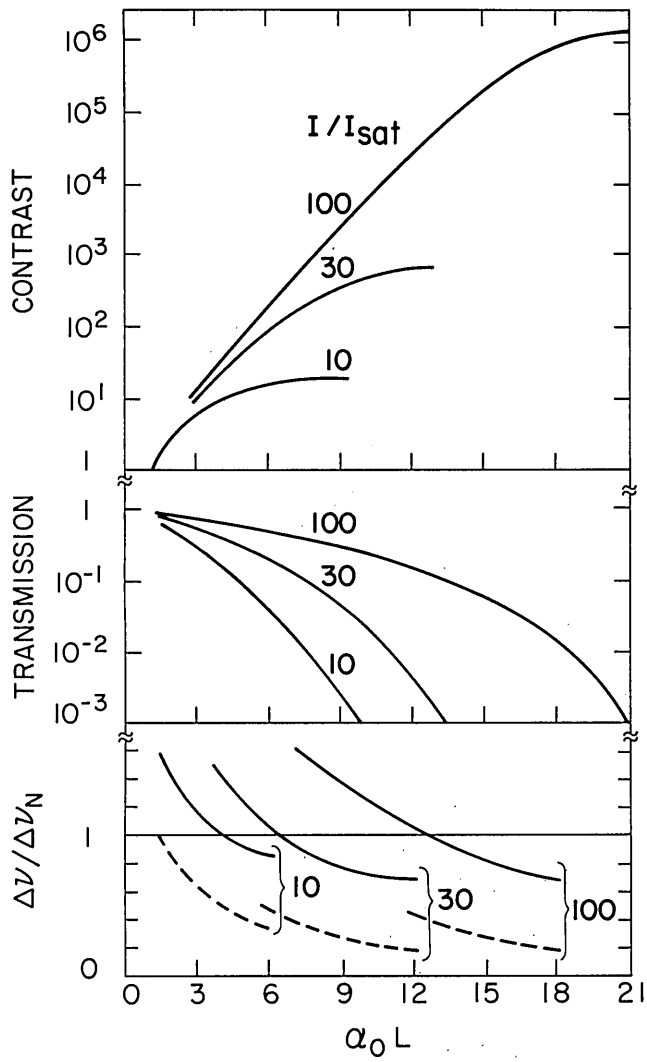

Fig. 3. Theoretical values for the contrast C, the probe-beam peak transmission T_0, and the Doppler-free signal half-width (solid lines) as functions of the integrated absorption lengths for different values of I/I_{sat}. The dashed lines show the theoretical linewidth for the tandem cell case.

According to this equation the attainable contrast increases from about 20 to about 2×10^6 when I/I_{sat} varies from 10 to 100, which is in accordance with the computer results in Fig. 3. Since the contrast is high in the regime studied, the probe peak transmission value T_0 is almost the same as the transmission of the Doppler-free signal (without background). In the lower part of the diagram the signal half-width, expressed in terms of the natural linewidth $\Delta\nu_N$, is plotted (solid lines). For a sample of low optical density a substantial power broadening is obtained. However, for more dense samples the wing absorption narrows down the linewidth and brings it down below the natural one. The details of the line-shape alteration are shown in Fig. 4 for different $\alpha_0 L$ values in the case of $I/I_{sat} = 30$. Here the Doppler-free signal amplitude has been normalized to 1. A Lorentzian corresponding to the natural line shape is indicated with a dashed line. The narrowing effect, related to the preferential wing absorption at increasing optical densities, can be clearly seen. It is interesting to note that, e.g., for $I/I_{sat} = 30$ the natural linewidth can be obtained with T as high as 12% and $C = 100$.

Experiments

Most of our experiments were performed on the sodium D_1 line ($3\,^2S_{1/2} - 3\,^2P_{1/2}$, $\lambda = 5896$ Å), using both experimental arrangements shown in Fig. 1. A Coherent Radiation Model 599-21 single-mode dye laser, pumped by an argon-ion laser, was used. This laser has a stabilized linewidth of about 1 MHz. An air track wavemeter was used to facilitate setting of the correct laser wavelength. Sodium cells of diameter 15 mm and of lengths up to 30 cm were used. Cells were placed in a piece of straight copper tubing wrapped with heating tape, and the temperature was measured with a thermocouple that was placed in contact with the cell. It is advantageous to use long cells in the present technique, since a high integrated absorption can then be obtained without operating at such a high vapor pressure that collisional broadening of the lines causes a serious problem. A simple silicon detector without any bias voltage was used to detect the transmitted beam. Frequently, strong attenuation filters had to be inserted in front of the detector in order to ensure operation in the linear regime. Laser beam diameters were typically 1 to 2 mm and were not determined accurately. The signals were recorded directly on an X-Y recorder synchronized with the slow laser wavelength sweep.

In Fig. 2, first examples of high-contrast recordings with the standard setup [Fig. 1(a)] are shown. Results from a detailed experimental investigation of the $F_{gr} = 1 - F_{exc} = 2$ line component [the highest-frequency component in Fig. 2(a)] are shown in Fig. 5. The primary pump power was 0.9 mW, and the probe-beam power was 0.004 mW. The signal intensity (probe-beam transmission), contrast, and linewidth are plotted. The data were obtained with a cell 30

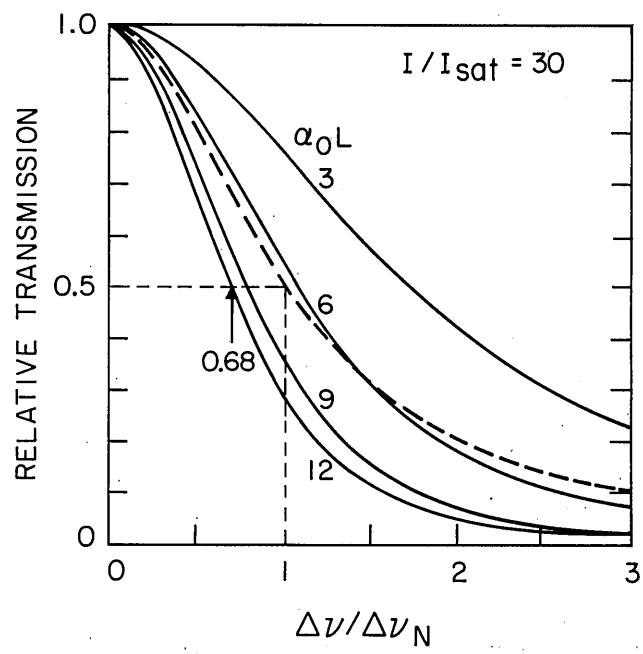

Fig. 4. Theoretical curves for the probe-beam transmission T for different absorption lengths $\alpha_0 L$. All curves are normalized to 1 at the line center. The dashed line corresponds to a Lorentzian with the natural linewidth.

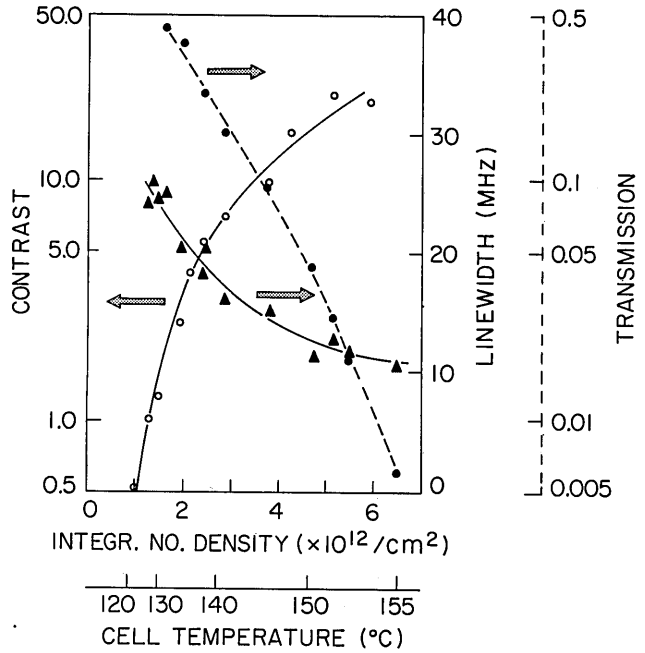

Fig. 5. Experimental results for the $F_{gr} = 1 - F_{exc} = 2$ component. Data were obtained with a 30-cm cell, using the arrangement given in Fig. 1(a) with 0.9 mW for the pump beam and 0.004 mW for the probe beam. ▲, Linewidth; ●, transmission.

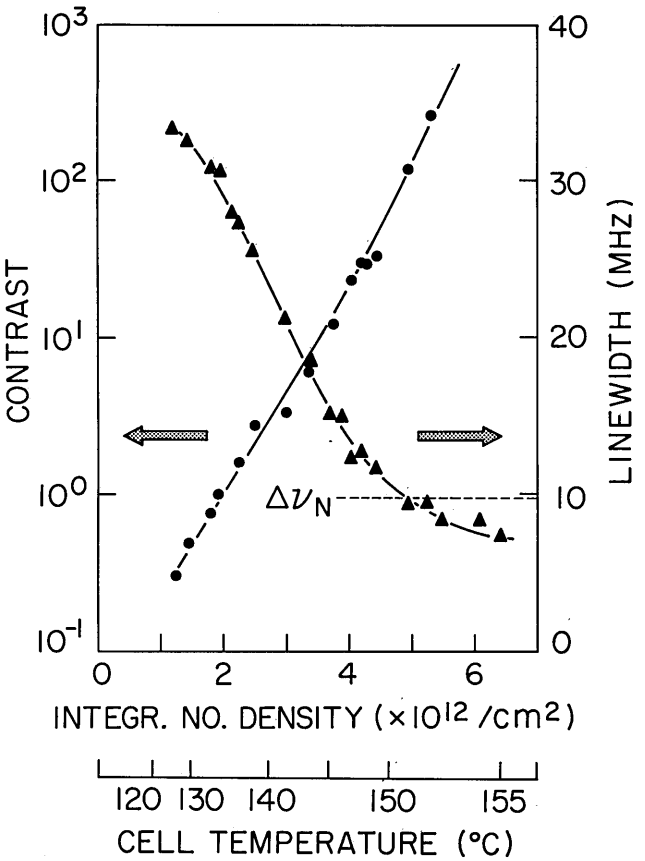

Fig. 6. Experimental results for the crossover signal connecting the $F_{gr} = 1$ level to the $F_{exc} = 2$ and $F_{exc} = 1$ levels. Data were obtained with a 30-cm cell in the arrangement shown in Fig. 1(b). The primary pump-beam power was 0.9 mW. Note the subnatural linewidth obtained.

cm long. As the signal goes to zero for very dense samples, a constant background level remains. This background is due to scattering of the pump light in the beam splitter in front of the detector and to fluorescence from the cell. Clearly, this background, which is incoherent, could be eliminated by spatial filtering or by moving the detector farther away. In calculating the contrast we have first subtracted the artificial background produced by the scattering. It can be seen that the contrast increases and the linewidth decreases for denser samples, as predicted by the curves in Fig. 3.

The sodium atom is clearly not a two-level system. The saturation is brought about by hyperfine pumping that depletes a particular lower level by pumping the atoms over into the other ground-state sublevel.[5] It is hard to estimate the effective value of I/I_{sat} for the transition studied. The data in Fig. 5 correspond roughly to the case $I/I_{sat} = 15$ for $\alpha_0 L$ values increasing up to 8. Detailed comparisons are not meaningful, since the experimental beams are Gaussian, whereas the theory was developed for "top-hat" beam profiles. The theory predicts linewidths below the natural one ($\Delta\nu_N = \frac{1}{2}\pi\tau = 9.7$ MHz[6] for our case), but this was not observed in this experiment, probably because of collision effects in the cell.

In our previous work,[1] detailed data were presented that had been obtained with the simplified arrangement shown in Fig. 1(b). Here we show instead corresponding data for the crossover signal connecting the $F_{exc} = 2$ and $F_{exc} = 1$ sublevels with the common $F_{gr} = 1$ level. Data for a cell 30 cm long are shown in Fig. 6. In this case extremely high contrasts (corrected for the constant-background level corresponding to about 0.003% transmission) are obtained, and linewidths well below the natural one are observed. The presented data match a I/I_{sat} value of about 35 and a $\alpha_0 L$ product increasing up to about 8. Since the probe beam in the case of the experimental arrangement of Fig. 1(b) is obtained from the pump beam after its passage through the cell, its primary intensity is not constant, as for the setup shown in Fig. 1(a). This means that the Doppler-free signal transmission in terms of the transmission (100%) measured when the laser is tuned completely off the line is lower than if the arrangement in Fig. 1(a) had been used. Since the transmission curves of Fig. 3 are given for the standard arrangement, we do not include the transmission data in Fig. 6. Note that the calculated values for the contrast and linewidth pertain to both experimental arrangements.

CASE OF SAMPLE REPUMPING

In saturation spectroscopy experiments in the regime of high integrated absorption discussed above, the intensity of the pump beam is strongly reduced when passing the sample. Thus it saturates much less efficiently in the back part of the cell than in its front part. (The intensity curve included in Fig. 1 is calculated for the case $I/I_{sat} = 30$ and $\alpha_0 L = 9$.) Thus the contrast obtained is mainly due to differences in transmission on and off resonance in the front path of the cell, whereas the back part is less active. This situation can be changed by focusing the pumping beam through the cell. However, the effect of keeping the pumping intensity high through the cell can more readily be demonstrated by injecting a second pump beam of the same intensity as the original

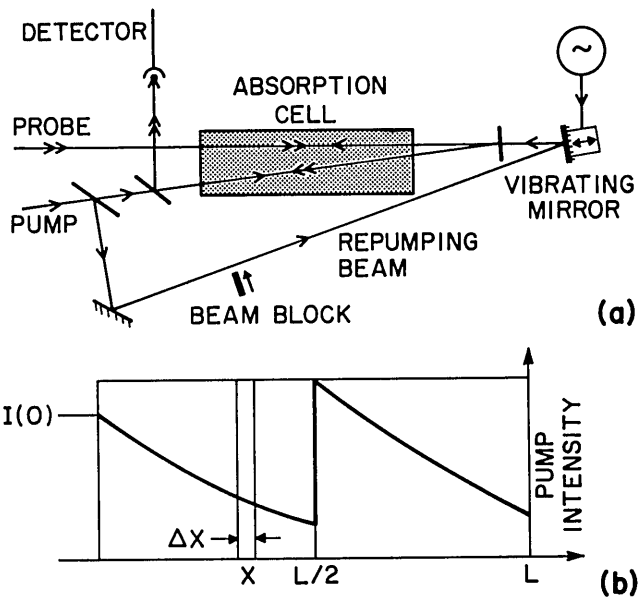

Fig. 7. (a) Arrangement for repumping experiments. (b) Diagram showing the pump-beam intensity through the double-passed cell in the presence or absence of a repumping beam of intensity equal as to that of the primary one. The curve was calculated for $I/I_{sat} = 30$ and $\alpha_0 L = 12$.

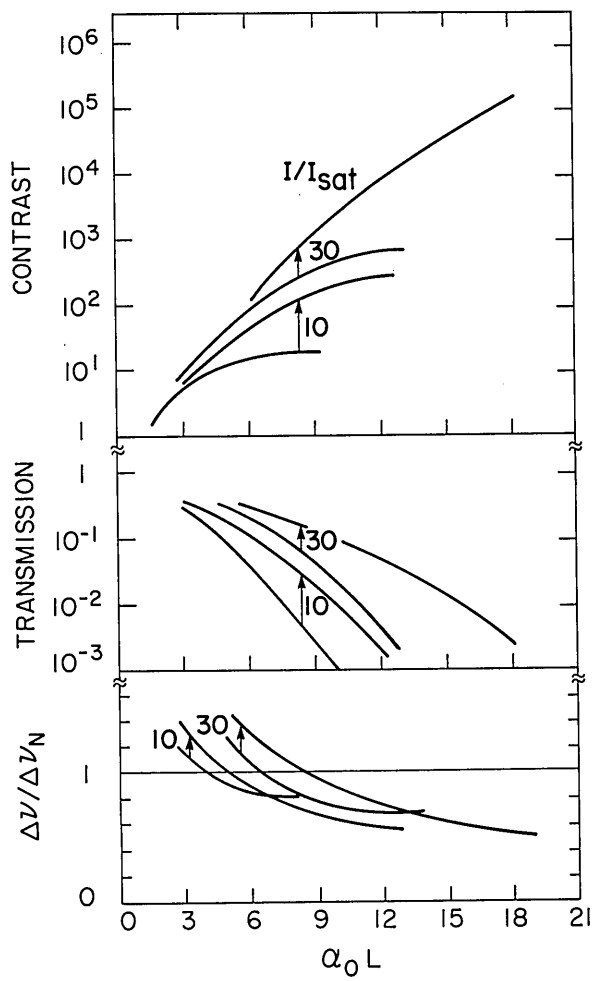

Fig. 8. Theoretical curves comparing the contrast, the transmission, and the linewidth for the cases of absence or presence of a repumping beam of intensity equal to that of the primary one. The arrows point toward the curves with repumping.

one after half the absorption path and observing the signal change when the repumping beam is blocked or unblocked.

A setup for achieving this is shown in Fig. 7(a). The absorption cell is double passed by the overlapping pump and probe beams that are folded after a first pass. By a mirror arrangement, additional pump-laser light is injected through the semitransparent folding mirror. This mirror has a high reflectivity so that it essentially folds only the primary light path without substantial intensity reduction. This means that most of the original pump-beam intensity must be used for the repumping-beam line. A vibrating mirror (mounted on a loudspeaker) is used in the repumping line in order to scramble the phase difference between the primary and the repumping beams and to avoid interference effects. The pump-beam intensity variation during the double pass is illustrated in Fig. 7(b) for selected experimental parameters. We have performed computer calculations for such a beam arrangement with the reinjection of a beam of the same intensity as the original beam. In Fig. 8, the transmission, the contrast, and the linewidth are shown for primary values of $I/I_{sat} = 10$ and $I/I_{sat} = 30$ in the cases of blocked and unblocked repumping lines ($\alpha_0 L$ is the value for double cell passes). It can be clearly seen how both transmission and contrast increase strongly when repumping is used. As expected, the effect is most drastic for strongly absorbing samples for which a linewidth reduction is also achieved. For weakly absorbing samples the linewidth increases, as expected, because of additional power broadening. To illustrate the effect of repumping, we note that for $I/I_{sat} = 10$ and a sample of a density corresponding to

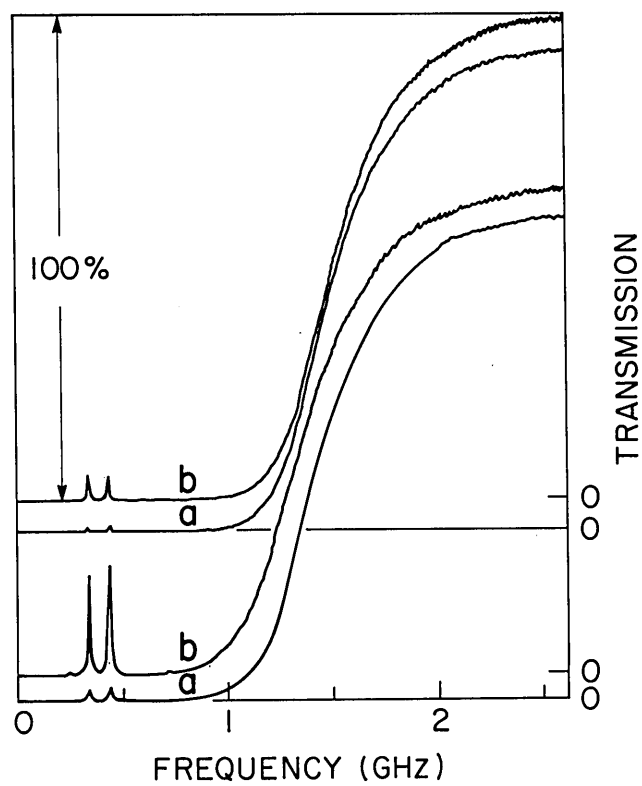

Fig. 9. Experimental curves for two slightly different cell temperatures, comparing the signals in (a) the absence and (b) the presence of a repumping beam. The temperature for the 30-cm cell was about 140°C. Primary and repumping beams both had a power of 1.6 mW, and that of the probe beam was 0.2 mW.

$\Delta\nu_{\text{normal}} = \Delta\nu_{\text{repump}} = 0.84\Delta\nu_N$ ($\alpha_0 L = 6.5$), T_0 is increased from 2.5 to 8% and C is increased from 16 to 60. For $I/I_{\text{sat}} = 30$ and $\Delta\nu_{\text{normal}} = \Delta\nu_{\text{repump}} = 0.68\ \Delta\nu_N$ ($\alpha_0 L = 13.8$), the increases are from 0.06 to 2.6% for T_0 and from 600 to 23,000 for C. Experimental curves obtained with an arrangement of the type illustrated in Fig. 7 are shown in Fig. 9. The strong increase in transmission induced by the repumping beam is very evident. Contrast is also enhanced, since the background level is unaffected by the additional pumping (apart from possible extra stray light).

CASE OF TANDEM ARRANGEMENT

As we have seen above, strong Doppler-free signals of high contrast can be obtained by using saturation spectroscopy in the regime of high linear absorption. This suggests a further type of experiment, in which extremely high-contrast conditions might be achieved simultaneously with drastic linewidth reductions beyond the natural radiation limit. A suggested experimental arrangement is shown in Fig. 10. It basically consists of two setups of the type shown in Fig. 1(b) in a series (tandem) arrangement. The first part can be considered a tunable laser source with Doppler-free atomic resonance output control. The schematic output of the source as a function of frequency is illustrated in Fig. 10, curve b, in accordance with the results given above. The output from this first setup is compressed by using an inverted beam expander in order to ensure that a sufficient power density can be achieved to saturate the transition in a second cell when the laser is tuned to the line center. However, since the primary pump-beam power for the second cell falls rapidly when the laser is tuned off the central frequency, its bleaching ability is strongly reduced in the wings. This leads to a much narrower saturation hole in the velocity distribution of the atoms in the second cell. The varying bleaching ability also leads to the narrowing of the frequency distribution of the pump-beam light penetrating the second cell (self-filtering: Fig. 10, curve c). However, this light is now used as the probe beam after backreflection. Thus the already spectrally narrowed probe-light intensity distribution is used to probe the narrowed saturation hole, leading to a much-narrowed transmission signal (Fig. 10, curve d). Basically, three nonlinear effects of exponential nature (comparing the conditions at the line center and in the line wings) are multiplied in the second-cell interaction, strongly narrowing the already spectrally narrow signal-beam frequency distribution that emerges from the first cell. The setups in Figs. 1(a) and 1(b) are equivalent with regard to signal linewidth and contrast for the first cell. However, this is not the case for the second-stage interaction because of the additional nonlinear spectral filtering of the pump beam (which will become the probe beam) passing through the second cell.

In order to calculate the resulting final signal characteristics, it is again necessary to consider the pump-beam attenuation through the cell. A numerical integration is again performed through the second cell for different frequency offsets from the center frequency. The intensity distribution obtained from the first cell is used as the input to calculate the resulting hole shape for the entire second cell. The emerging pump-beam intensity distribution is calculated and is linearly convolved with the cell transmission characteristics for the (weak) probe beam. The results of a linewidth calculation for I/I_{sat} values of 10, 30, and 100 assigned to the first-cell pump beam and to the line-center intensity of the compressed pump beam in the second cell are included as dashed lines in the lower part of Fig. 3. Linewidths reduced to a small fraction of the natural one are predicted. In the tandem arrangement, contrast values higher than the square of the single-cell contrast values are obtained, yielding truly extreme values. The line shape dependence on the I/I_{sat} value at the line center for the second-cell pump beam is illustrated in Fig. 11 with $\alpha_0 L = 6$ for both the first and the second cells and $I/I_{\text{sat}} = 10$ for the first-cell pump beam. As a further illustration, the influence of successive heating of the second cell is shown in Fig. 12 with $I/I_{\text{sat}} = 10$ in both cells and $\alpha_0 L = 4.5$ for the first cell.

It can be noted that the repumping case is equivalent to the tandem case, apart from the important difference that

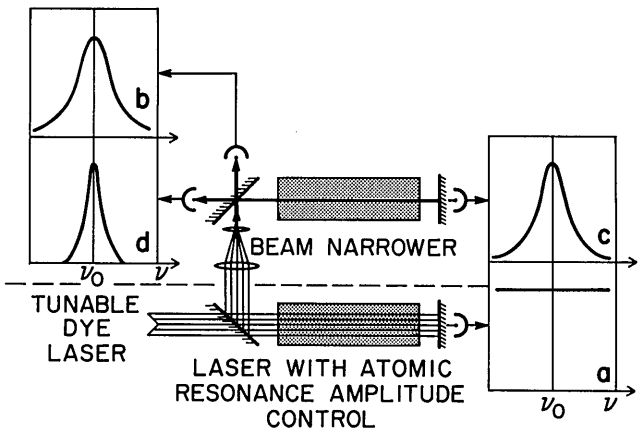

Fig. 10. The principle of tandem transmission spectroscopy. Curves a–d show the line shape at different positions in the setup.

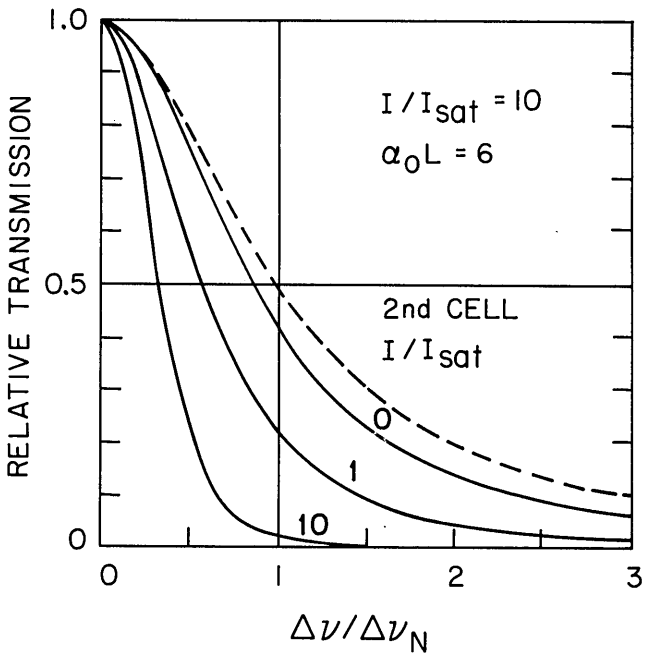

Fig. 11. Theoretical curves for the transmission signal for increasing values of the saturation parameter for the second cell. All curves are normalized to 1. The first-cell parameters are $I/I_{\text{sat}} = 10$ and $\alpha_0 L = 6$, corresponding to $T_0 = 0.041$ and $C = 15.4$. A natural-linewidth Lorentzian is included as a dashed-line curve.

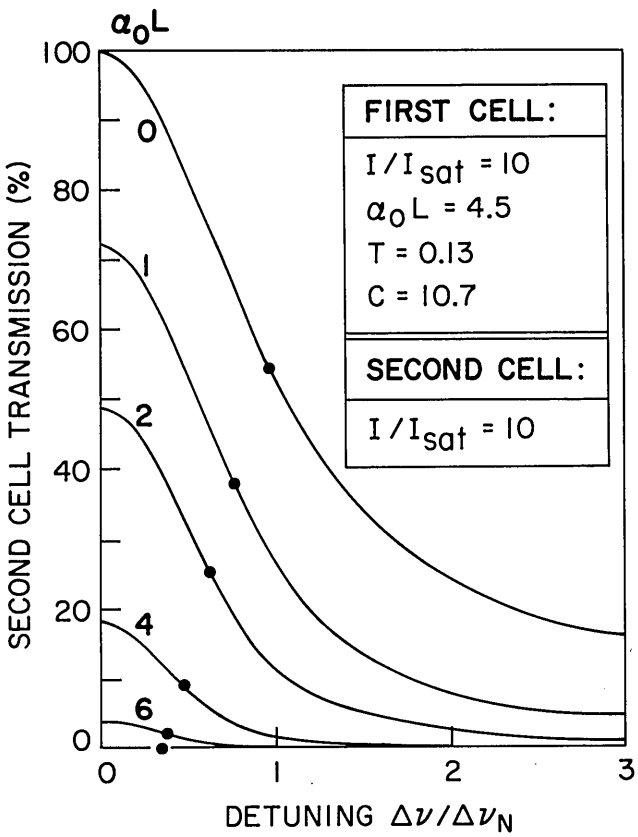

Fig. 12. Theoretical curves showing the effect of heating the second cell for other (given) parameters. The transmission, normalized to 100% for an empty second cell, is reduced when the second cell starts to absorb, and at the same time a strong line narrowing is expected.

the second stage in the former case utilizes a constant-power pump beam and a detuning-dependent probe beam, whereas detuning-dependent beams in the latter setup are used for both pumping and probing. Since much unused laser power is available for second-stage pumping in the repumping setup, such experiments can easily be performed as illustrated above. For the more drastic tandem case the detuning-dependent second-cell pump power is substantial but still quite restricted, and great care must be exercised in the experimental realization of this scheme. So far, tandem experiments have not been performed.

DISCUSSION

The high-contrast transmission experiments discussed in this paper feature drastic values for transmission, contrast, and linewidth. These conditions are obtained by working in the little-explored region of high saturating powers and high integrated sample absorption. By using simplifying assumptions, straightforward theoretical explanations of the observed phenomena can be given. The ac Stark effect has been neglected in our calculations. The influence of this effect seems to be small in the high-contrast regime, which at first sight seems surprising. However, the hole burned then has a sharp, unshifted part because of the cell region where the pump beam has become strongly attenuated. A study of possible shifts in the positions of the narrowed line components will be reported separately.[7]

The narrowing of signal components below the natural radiation limit in experiments of this kind is an interesting feature. Tandem-type experiments with predicted extremely sharp lines should be feasible if a high-power single-mode ring laser is used and if a suitable geometrical arrangement can be found for the beams through the first cell, permitting use of a large beam cross section while avoiding detrimental effects of spatial hyperfine pumping.

It should be pointed out that close-lying, normally unresolved components are not expected to resolve within the theoretical model used for describing the high-contrast experiments. The influence of multiple-scattering effects in this context is still to be explored. The sharp and strong signals obtainable with extremely simple arrangements might prove to be very useful for locking lasers to an atomic line. The arrangement in Fig. 1(b) could provide most of the laser output for external use through reflection off the beam splitter, whereas only a small fraction is passed through the beam splitter and used for spectroscopic locking purposes.

By directing the backreflected beam at a small angle to, but still partially overlapping with, the primary beam, Doppler-free deflection signals can be obtained.[8] By using a split detector, dispersion-shaped signals particularly suitable for electronic locking can be obtained. In the high-contrast regime the deflection experiments also provide strong signals, since the deflections are enhanced by the strong index gradients. Successful Doppler-free deflection experiments were actually performed for the sodium *D* lines.

Simple and cheap spectroscopic techniques are of particular interest to match the cheap single-mode room-temperature diode lasers that now are available for use in the near-infrared region.[9] The strong resonance lines of K (767 nm, 770 nm), Rb (780 nm, 795 nm) and Cs (852 nm, 894 nm) are well suited for frequency-stabilizing puposes by using the present technique.

Experiments in the time domain employing the high-contrast regime of saturation spectroscopy might reveal interesting switching behavior and possibly optical bistability.[10] In particular, counterpropagating beams of equal intensity penetrating a cell with added buffer gas should feature temporal hysteresis effects at the line center.

ACKNOWLEDGMENTS

This work was supported in part by the U.S. Office of Naval Research under contract ONR N00014-C-78-0403 and in part by the National Science Foundation under contract PHY-83-08271.

S. Svanberg is on sabbatical from the Lund Institute of Technology, Sweden.

G.-Y. Yan is on leave from East China Normal University, Shanghai, China.

* Permanent address: Beijing Normal University, China.

REFERENCES

1. S. Svanberg, G.-Y. Yan, T. P. Duffey, and A. L. Schawlow, Opt. Lett. **11**, 138 (1986).
2. T. W. Hänsch, I. S. Shahin, and A. L. Schawlow, Phys. Rev. Lett. **27**, 707 (1971).
3. T. W. Hänsch and P. Toschek, Z. Phys. **236**, 213 (1970).

4. C. Wieman and T. W. Hänsch, Phys. Rev. Lett. **36,** 1170 (1976).
5. P. G. Pappas, M. M. Burns, D. D. Hinshelwood, M. S. Feld, and D. E. Murnick, Phys. Rev. A **21,** 1955 (1980).
6. A. Gaupp, P. Kuske, and W. Wittman, Phys. Rev. A **26,** 3351 (1982).
7. W.-X. Peng, A. Persson, and L. Sturesson, Department of Physics, Lund Institute of Technology, Lund, Sweden (personal communication).
8. B. Couillaud and A. Ducasse, Phys. Rev. Lett. **35,** 1276 (1975).
9. J. C. Camparo, Contemp. Phys. **24,** 443 (1985).
10. H. M. Gibbs, *Optical Bistability: Controlling Light with Light* (Academic, New York, 1986).